CRACK-TIP FIELDS FOR FAST FRACTURE
OF AN ELASTIC-PLASTIC MATERIAL

by

J. D. Achenbach
Department of Civil Engineering
Northwestern University
Evanstown, Illinois

M. F. Kanninen
Applied Solid Mechanics Section
Battelle
Columbus, Ohio

and

C. H. Popelar
Engineering Mechanics Department
The Ohio State University
Columbus, Ohio

December, 1979

ADA085261

LEVEL II

DTIC
ELECTED
JUN 10 1980
D

80   6 6   0 80

SECURITY CLASSIFICATION OF THIS PAGE (When Data Entered)

REPORT DOCUMENTATION PAGE		READ INSTRUCTIONS BEFORE COMPLETING FORM
1. REPORT NUMBER	2. GOVT ACCESSION NO. AD-A085261	3. RECIPIENT'S CATALOG NUMBER
4. TITLE (and Subtitle) CRACK-TIP FIELDS FOR FAST FRACTURE OF AN ELASTIC-PLASTIC MATERIAL .		5. TYPE OF REPORT & PERIOD COVERED Interim rept. 6. PERFORMING ORG. REPORT NUMBER
7. AUTHOR(s) J. D. Achenbach, M. F. Kanninen, and C. H. Popelar		8. CONTRACT OR GRANT NUMBER(s) N00014-76-C-0063 (Northwestern) N00014-77-C-0576 (Battelle)
9. PERFORMING ORGANIZATION NAME AND ADDRESS Northwestern University, Evanston, Ill, 60201 and Battelle, Columbus, Ohio 43201 and The Ohio State University, Columbus, Ohio 43201		10. PROGRAM ELEMENT, PROJECT, TASK AREA & WORK UNIT NUMBERS
11. CONTROLLING OFFICE NAME AND ADDRESS Office of Naval Research Structural Mechanics Program Dept. of the Navy, Arlington, VA 22217		12. REPORT DATE December 1979 13. NUMBER OF PAGES 33
14. MONITORING AGENCY NAME & ADDRESS(If different from Controlling Office)		15. SECURITY CLASS. (of this report) Unclassified 15a. DECLASSIFICATION/DOWNGRADING SCHEDULE

16. DISTRIBUTION STATEMENT (of this Report)

Approved for public release; distribution unlimited

17. DISTRIBUTION STATEMENT (of the abstract entered in Block 20, if different from Report)

18. SUPPLEMENTARY NOTES

Submitted for publication in the Journal of the Mechanics and Physics of Solids

19. KEY WORDS (Continue on reverse side if necessary and identify by block number)

near tip stress field   crack arrest
rapid crack propagation
fracture toughness
elastic-plastic material

20. ABSTRACT (Continue on reverse side if necessary and identify by block number)

An asymptotic analysis of the near-tip fields is given for transient crack propagation in an elastic-plastic material. The material is characterized by J_2 flow theory together with a bilinear effective stress-strain curve. Both plane stress and plane strain conditions have been considered. Explicit results are given for the order of the crack-tip singularity, the angular position at which unloading occurs, and the angular variation of the near-tip stresses, all as functions of the crack-tip speed and the ratio of the slopes of the two portions of the bilinear stress-strain relation.

DD FORM 1473 EDITION OF 1 NOV 65 IS OBSOLETE
1 JAN 73
S/N 0102-LF-014-6601

SUMMARY

An asymptotic analysis of the near-tip fields is given for transient crack propagation in an elastic-plastic material. The material is characterized by J_2 flow theory together with a bilinear effective stress-strain curve. Both plane stress and plane strain conditions have been considered. Explicit results are given for the order of the crack-tip singularity, the angular position at which unloading occurs, and the angular variation of the near-tip stresses, all as functions of the crack-tip speed and the ratio of the slopes of the two portions of the bilinear stress-strain relation.

p. i

CRACK TIP FIELDS FOR FAST FRACTURE
OF AN ELASTIC-PLASTIC MATERIAL

by

J. D. Achenbach, M. F. Kanninen, and C. H. Popelar

INTRODUCTION

An expanding interest is developing in the analysis of rapid
unstable crack propagation in which dynamic (inertia) effects may not be
negligible. While this interest has been motivated in part by intellectual
curiosity in a new and fertile applied mechanics research area, there is
also a growing realization that many engineering applications for this
technology exist. There are many practical situations in which the result
of large scale unstable crack growth is completely unacceptable. To pre-
clude such catastropic occurrences, it is important to develop treatments
for the arrest of rapid crack propagation. Because crack arrest must
logically be viewed as the termination of fast fracture, attention must
be focused on the dynamic crack propagation process.

For the most part, dynamic fracture mechanics is now based upon
elastodynamic solutions; for example, see Kanninen (1978). Yet, most struc-
tural components where fracture is a concern employ tough ductile materials
where it is unlikely that the basic assumptions of linear elastic fracture
mechanics (LEFM) are valid. In addition, recent work has begun to raise
serious questions about the extent to which the dynamic fracture toughness
is truly a material property, even when LEFM conditions are satisfied.
Thus, it is necessary to develop nonlinear dynamic elastic-plastic frac-
ture mechanics treatments.

Because unloading may take place in dynamic crack propagation, a deformation theory formulation is undesirable. A flow theory approach is required to account for the elastic unloading in the wake of the crack tip. An asymptotic solution near the tip of a crack propagating dynamically in antiplane strain (Mode III) conditions using such an approach has already been given by Achenbach and Kanninen (1978). Their results determined the form of the crack tip singularity and the angular position at which elastic unloading commences. Clearly, this kind of information is needed in order to devise a finite element or other solution procedure for dynamic crack propagation and arrest analyses.

The work described in this paper extends the Achenbach-Kanninen approach to Mode I crack growth. Results for both plane stress and plane strain conditions are given. These solutions are based upon J_2 flow theory with a bilinear stress-strain relation which allows elastic unloading. The problem formulation leads to a nonlinear eigenvalue problem which is solved using an iterative numerical solution procedure. Confidence in the results was attained by comparisons with the results obtained by Amazigo and Hutchison (1977) for the special case of quasi-static crack growth at low crack-tip speeds when the dynamic effects are negligible.

THE SOLUTION PROCEDURE

Problem Formulation

The fields of stress and deformation are referred to a coordinate system whose origin is attached to the moving crack tip. The system of coordinates is shown in Figure 1. The crack is located in the $(x_1 x_3)$-plane where the x_3 axis coincides with the crack front and x_1 is the direction of crack advance. The relevant displacement components are $u_1(x_1, x_2, t)$ and $u_2(x_1, x_2, t)$, where t is time.

In the following the material derivatives with respect to time will frequently be needed. These are defined as

$$(\dot{\ }) = \frac{\partial}{\partial t} - v(t) \frac{\partial}{\partial x_1} \tag{1}$$

$$(\ddot{\ }) = \frac{\partial^2}{\partial t^2} - \dot{v}(t) \frac{\partial}{\partial x_1} - 2v(t) \frac{\partial^2}{\partial x_1 \partial t} + [v(t)]^2 \frac{\partial^2}{\partial x_1^2} \tag{2}$$

where $v(t)$ is the speed of the crack tip. Notice that v need not be constant and is only subject to the conditions that $v(t)$ and dv/dt are continuous functions.

For the case of plane stress, the non-vanishing stress components are σ_{11}, $\sigma_{12} = \sigma_{21}$, and σ_{22}. The equations of motion are of the form

$$\sigma_{\gamma\delta,\delta} = \rho \ddot{u}_\gamma \ ; \qquad \gamma, \delta = 1, 2 \tag{3}$$

where the second-order material time-derivative is defined by (2)*.

The constitutive equations in the elastic-plastic material take into account strain-hardening characterized by J_2 flow theory and a bilinear effective

---

*In the following, Greek minuscules have the values 1,2 whereas Latin minuscules have the values 1,2,3.

stress-strain curve. This curve is shown in Figure 2. Let σ_o denote the
yield stress in tension, E Young's modulus, and $\alpha = E_t/E$, where E_t is the
slope of the bilinear stress-strain relation in tension for stresses in excess
of σ_o. The effective stress is defined as

$$\sigma_e = (\tfrac{3}{2} s_{ij} s_{ij})^{1/2} \tag{4}$$

where s_{ij} is the stress deviator. The constitutive relations for an elasti-
cally isotropic solid may then be written following Amazigo and Hutchinson
(1977):

loading ($\dot\sigma_e \geq o$):

$$E_t \dot\epsilon_{ij} = \alpha[(1 + \nu)\dot\sigma_{ij} - \nu\dot\sigma_{kk}\delta_{ij}] + (\tfrac{3}{2} \sigma_e)(1 - \alpha)s_{ij}\dot\sigma_e \tag{5}$$

unloading ($\dot\sigma_e < o$):

$$E_t\dot\epsilon_{ij} = \alpha[(1 + \nu)\dot\sigma_{ij} - \nu\dot\sigma_{kk}\delta_{ij}] \tag{6}$$

where ν is Poisson's ratio.

Field Equations for a Near-Tip Analysis

In this paper, certain a-priori assumptions are made with respect to
the general nature of the deformation in the immediate vicinity of the crack tip.
Explicit expressions for the near-tip fields will be derived using these assump-
tions. It will then be shown that the required boundary and continuity condi-
tions are satisfied.

It is assumed that ahead of the crack tip a plastic loading zone
exists which is bounded in the near-tip region by radial lines emanating from

the crack tip at angles $\theta = \pm\theta_p$. This is shown in Figure 1. An elastic unloading zone is assumed for $|\theta| > \theta_p$. The possible presence of a plastic reloading zone for $|\theta|$ near π is neglected in this paper. Conceptually, it is possible to include such a reloading zone. But, just as for the quasi-static case investigated by Amazigo and Hutchinson (1977), it is expected that the influence of reloading is not significant enough to justify the computational complications that would be required to treat it.

In the plastic loading zone, asymptotic solutions near the crack tip of the general form

$$\dot{u}_\gamma = K v \dot{U}_\gamma(\theta) \, r^s \qquad (7)$$

are sought. Here, K is an amplitude factor, while $\dot{U}_\gamma(\theta)$ and s are to be determined. In an asymptotic analysis, only the lowest orders in r need to be retained. This means that $\partial/\partial t$ can be neglected compared to $-v(t)\partial/\partial x_1$ in (1). Thus

$$(\dot{}) \sim - v(t) \frac{\partial}{\partial x_1} \qquad (8)$$

By using the relations

$$\frac{\partial}{\partial x_1} = \cos\theta \, \frac{\partial}{\partial r} - \frac{\sin\theta}{r} \frac{\partial}{\partial \theta} \qquad (9)$$

and

$$\frac{\partial}{\partial x_2} = \sin\theta \, \frac{\partial}{\partial r} + \frac{\cos\theta}{r} \frac{\partial}{\partial \theta} \qquad (10)$$

the strain rates corresponding to (7) are then computed as

$$\dot{\epsilon}_{11} = K \, v \, [s \, \dot{U}_1 \cos\theta - \dot{U}_1' \sin\theta] \, r^{s-1} \tag{11}$$

$$\dot{\epsilon}_{22} = K \, v \, [s \, \dot{U}_2 \cos\theta + \dot{U}_2' \cos\theta] \, r^{s-1} \tag{12}$$

$$\dot{\epsilon}_{12} = \frac{1}{2} K \, v \, [s \, \dot{U}_1 \sin\theta + \dot{U}_1' \cos\theta + s \, \dot{U}_2 \cos\theta - \dot{U}_2' \sin\theta] \, r^{s-1} \tag{13}$$

where $(\ )' = d/d\theta$. Also by definition

$$\{\sigma_{ij}, \ \sigma_e, \ s_{ij}\} = K \, E \, \{\Sigma_{ij}(\theta), \ \Sigma_e(\theta), \ S_{ij}(\theta)\} \, r^s \tag{14}$$

and

$$\{\dot{\sigma}_{ij}, \ \dot{\sigma}_e, \ \dot{s}_{ij}\} = K \, E \, v \, \{\dot{\Sigma}_{ij}(\theta), \ \dot{\Sigma}_e(\theta), \ \dot{S}_{ij}(\theta)\} \, r^{s-1} \tag{15}$$

By virtue of (8) and (9), the following relation holds

$$\dot{\Sigma}_{ij} = s \Sigma_{ij} \cos\theta + \Sigma_{ij}' \sin\theta \tag{16}$$

Analogous relations hold for $\dot{\Sigma}_e(\theta)$ and $S_{ij}(\theta)$. Also

$$S_{ij} = \Sigma_{ij} - \frac{1}{3} \Sigma_{kk} \, \delta_{ij} \tag{17}$$

$$\Sigma_e = (\frac{3}{2} S_{ij} S_{ij})^{1/2} \tag{18}$$

By substituting (7) and the first of (14) into the equations of motion (3), we obtain in the plastic loading zone near the crack-tip

$$s \, \Sigma_{11} \cos\theta - \Sigma_{11}' \sin\theta + s \, \Sigma_{21} \sin\theta + \Sigma_{21}' \cos\theta = \beta^2 (-s \, \dot{U}_1 \cos\theta + \dot{U}_1' \sin\theta) \tag{19}$$

$$s \, \Sigma_{12} \cos\theta - \Sigma_{12}' \sin\theta + s \, \Sigma_{22} \sin\theta + \Sigma_{22}' \cos\theta = \beta^2 (-s \, \dot{U}_2 \cos\theta + \dot{U}_2' \sin\theta) \tag{20}$$

where

$$\beta = v/c, \qquad c = (E/\rho)^{1/2} . \tag{21}$$

Substitution of (11) through (18) into the constitutive relations (5) and (6) yields

$$\alpha \left[s \, \dot{U}_1 \cos\theta - \dot{U}_1' \sin\theta \right] = \alpha \left[(1+\nu) \, \dot{\Sigma}_{11} - \nu \dot{\Sigma}_{kk} \right] + \frac{3}{2} (1-\alpha) \, \Sigma_e^{-1} S_{11} \, \dot{\Sigma}_e \qquad (22)$$

$$\alpha \left[s \, \dot{U}_2 \sin\theta + \dot{U}_2' \cos\theta \right] = \alpha \left[(1+\nu) \, \dot{\Sigma}_{22} - \nu \dot{\Sigma}_{kk} \right] + \frac{3}{2} (1-\alpha) \, \Sigma_e^{-1} S_{22} \, \dot{\Sigma}_e \qquad (23)$$

$$\alpha \left[s \, \dot{U}_1 \sin\theta + \dot{U}_1' \cos\theta + s \, \dot{U}_2 \cos\theta - \dot{U}_2' \sin\theta \right] = 2 \, \alpha \, (1+\nu) \, \dot{\Sigma}_{12}$$
$$+ 3 \, (1-\alpha) \, \Sigma_e^{-1} \Sigma_{12} \, \dot{\Sigma}_e \qquad (24)$$

The unknowns in these equations are U_γ and $\dot{\Sigma}_{\gamma\delta}$.

The above formulation was derived for plane stress conditions. For the case of plane strain, we have the condition $\dot{\varepsilon}_{33} = 0$ and the nonvanishing stress σ_{33}. It follows from (5) and (14) that the additional relation required for determining Σ_{33} is

$$\alpha \left[(1 + \nu) \, \dot{\Sigma}_{33} - \nu \dot{\Sigma}_{kk} \right] + \frac{3}{2} (1 - \alpha) \, \Sigma_e^{-1} S_{33} \, \dot{\Sigma}_e = 0 \qquad (25)$$

No other changes are needed.

Corresponding equations for the elastic unloading region can be obtained from the work of Achenbach and Bazant (1975). In the elastic region the displacement rate must satisfy for plane strain the equation

$$(\lambda + \mu)\dot{u}_{\gamma,\gamma\delta} + \mu\dot{u}_{\delta,\gamma\gamma} = \rho u_\delta^{\cdot\cdot} \qquad (26)$$

where λ and μ are Lame's elastic constants. We introduce the displacement-rate potentials $\dot{\phi}$ and $\dot{\psi}$ through

$$\dot{u}_1 = \frac{\partial \dot{\phi}}{\partial x_1} + \frac{\partial \dot{\psi}}{\partial x_2} ; \qquad \dot{u}_2 = \frac{\partial \dot{\phi}}{\partial x_2} - \frac{\partial \dot{\psi}}{\partial x_1} \tag{27}$$

It is then not difficult to show that $\dot{u}_1$ and $\dot{u}_2$ will satisfy (26) if $\dot{\phi}$ and $\dot{\psi}$ are solutions of the wave equations

$$\dot{\phi},_{\gamma\gamma} = \frac{1}{c_L^2} (\dot{\phi})^{\cdot\cdot} ; \qquad c_L^2 = (\lambda + 2\mu)/\rho \tag{28}$$

$$\dot{\psi},_{\gamma\gamma} = \frac{1}{c_T^2} (\dot{\psi})^{\cdot\cdot} ; \qquad c_T^2 = \mu/\rho \tag{29}$$

In the near-tip region, the stresses in the elastic unloading zone may be expressed in terms of $\dot{\phi}$ and $\dot{\psi}$ by

$$-\nu\mu^{-1}\sigma_{22} = \beta_T^2 \frac{\partial \dot{\phi}}{\partial x_1} - (\frac{\partial \dot{\phi}}{\partial x_1} + \frac{\partial \dot{\psi}}{\partial x_2}) \tag{30}$$

$$-\nu\mu^{-1}\sigma_{21} = 2 \frac{\partial \dot{\phi}}{\partial x_2} + (\beta_T^2 - 2) \frac{\partial \dot{\psi}}{\partial x_1} \tag{31}$$

where we have used (8).

Let us now consider solutions of (28) and (29) of the general forms

$$\dot{\phi} = K v \dot{\phi}(\beta_L, \epsilon) r^P, \qquad \beta_L = v(t)/c_L \tag{32}$$

$$\dot{\psi} = K v \dot{\psi}(\beta_T, \theta) r^P, \qquad \beta_T = v(t)/c_T \tag{33}$$

Solutions of this kind follow immediately as a slight generalization of Equations (22) and (23) of Achenbach and Bazant (1975) as

$$\dot{\phi}(\beta_L^2, \theta) = (1 - \beta_L^2 \sin^2\theta)^{P/2} [A \sin\rho(\epsilon - \pi) + B \cos\rho(\epsilon - \pi)] \tag{34}$$

9

$$\dot{\Psi}(\beta_T^2, \theta) = (1 - \beta_T^2 \sin^2 \theta)^{P/2} [C \sin\rho(\omega - \pi) + D \cos\rho(\omega - \pi)] \qquad (35)$$

where

$$\tan \omega = (1 - \beta_L^2)^{1/2} \tan\theta \qquad (36)$$

$$\tan \varepsilon = (1 - \beta_T^2)^{1/2} \tan\theta \qquad (37)$$

Defining

$$\dot{u}_\gamma = K \, v \, \dot{U}_\gamma^{el}(\theta) r^{P-1} \qquad (38)$$

we find the following relations on the basis of (27) and (9-10)

$$\dot{U}_1^{el} = p \cos\theta \, \dot{\Phi} - \sin\theta \, \dot{\Phi}' + p \sin\theta \, \dot{\Psi} + \cos\theta \, \dot{\Psi}' \qquad (39)$$

$$\dot{U}_2^{el} = p \sin\theta \, \dot{\Phi} + \cos\theta \, \dot{\Phi}' - p \cos\theta \, \dot{\Psi} + \sin\theta \, \dot{\Psi}' \qquad (40)$$

The governing equations for conditions of plane stress in the elastic region can be obtained from the above by replacing λ by $\mu/(1 - \nu)$.

Boundary Conditions

The governing equations in the plastic loading zone, (19) through (24), and the general forms of the solutions in the elastic unloading zone, (34) through (40), must be supplemented by boundary conditions at $\theta = 0$ and $\theta = \pi$, and continuity conditions at $\theta = \theta_p$. By virtue of symmetry, the following conditions hold at $\theta = 0$.

$$\dot{U}_2 = 0 \qquad (41)$$

$$\Sigma_{12} = 0 \qquad (42)$$

$$\dot{U}_1' = 0 \qquad (43)$$

Equations (30) and (31) together with the conditions that σ_{21} and σ_{22} vanish at $\theta = \pi$ yield the following relations

10

$$(\beta_T^2 - 2)\, pB - 2p\,(1 - \beta_T^2)^{1/2}\, C = 0 \qquad (44)$$

$$2p\,(1 - \beta_L^2)^{1/2}\, A + (\beta_T^2 - 2)p\, D = 0 \qquad (45)$$

Thus, the displacements and the stresses in the elastic unloading zone can be expressed in terms of two unknown constants, say A and B.

Now, consider the conditions at $\theta = \theta_p$. An obvious condition follows by comparison of (7) and (38) as

$$s = p - 1 \qquad (46)$$

Since $\theta = \theta_p$ separates the plastic loading zone from the elastic unloading zone, $\dot{\sigma}_e$ must vanish there. This implies that $\dot{\Sigma}_e$ vanishes at $\theta = \theta_p$; i.e.,

$$-s\,\Sigma_e\cos\theta + \Sigma_e'\sin\theta = 0 \qquad (47)$$

Continuity of traction-rates across $\theta = \theta_p$ requires that

$$[\dot{\Sigma}_\theta] = 0 \text{ and } [\dot{\Sigma}_{\theta r}] = 0 \qquad (48)$$

Here the following notation has been used

$$[\ ] = \lim_{\theta \to \theta_p^+}(\ ) - \lim_{\theta \to \theta_p^-}(\ ) \qquad (49)$$

Displacement-rates are also continuous at $\theta = \theta_p$. Consequently,

$$[\dot{U}_r] = [\dot{U}_\theta] = [\dot{U}_1] = [\dot{U}_2] \equiv 0 \qquad (50)$$

Since $[\dot{U}_r] = 0$, we have $[\dot{\epsilon}_r] = 0$. Then, since $\dot{\Sigma}_e = 0$ and $[\dot{\Sigma}_\theta] = 0$, it follows

from (5) and (6) that $[\dot{\Sigma}_r] = 0$. This result, together with (48), implies $[\delta_{\gamma\delta}] = 0$. From this it follows that $[\dot{\varepsilon}_{\gamma\delta}] = 0$. Since the strain rates and the displacement-rates are continuous, it follows from (11) through (13) that

$$[\dot{U}_1'] = [\dot{U}_2'] = 0 \qquad (51)$$

at $\theta = \theta_p$.

Since explicit expressions for the fields in the elastic unloading zone are available, the continuity conditions (50) and (51) can be used to generate boundary conditions for the domain $0 \le \theta \le \theta_p$. The two unknown constants in the unloading zone, A and B, can be expressed in terms of $U_1(\theta_p^-)$ and $\dot{U}_2(\theta_p^-)$ by the use of (49). Next, the quantities $(\dot{U}_1^{el})$ and $(\dot{U}_2^{el})$, which are now in terms of $\dot{U}_1(\theta_p^-)$, $\dot{U}_2(\theta_p^-)$, s, θ_p, β_L and β_T are computed and the continuity conditions (50) imposed. This yields general relations of the forms

$$\dot{U}_1'(\theta_p^-) = a_{11}(s,\theta_p)\, \dot{U}_1(\theta_p^-) + a_{12}(s,\theta_p)\, \dot{U}_2(\theta_p^-) \qquad (52)$$

$$\dot{U}_2'(\theta_p^-) = a_{21}(s,\theta_p)\, \dot{U}_1(\theta_p^-) + a_{22}(s,\theta_p)\, \dot{U}_2(\theta_p^-) \qquad (53)$$

The functions $a_{\gamma\delta}(s,\theta_p)$, which also depend on β_L and β_T, are rather lengthy, and they are not reproduced here.

Numerical Solution

Equations (47), (52), and (53) provide a set of boundary conditions for the domain $0 \le \theta \le \theta_p$. The governing equations for this domain are given by (19) through (24). The boundary conditions at $\theta = 0$ are given by (41) through (43). The unknowns are the functions depending on θ, such as $\dot{U}_1(\theta)$, etc, as well as the values of θ_p and s. The problem defined in this manner is

like a nonlinear eigenvalue problem, similar to, but more complicated than the one discussed for the anti-plane case by Achenbach and Kanninen (1978). The problem must be solved numerically as discussed in this section.

When (16) is used to eliminate $\dot{\Sigma}_{ij}$ in (19) through (24) and (47), the latter can be written in matrix form as

$$\underset{\sim}{D}(S_{ij}) \, \underset{\sim}{y} + \underset{\sim}{R} \, \underset{\sim}{y} = 0 \qquad (54)$$

where

$$\underset{\sim}{y}^T = [\dot{U}_1, \ \dot{U}_2, \ \Sigma_{11}, \ \Sigma_{22}, \ \Sigma_{12}, \ \Sigma_{33}] \qquad (55)$$

in which the superscript T denotes the transpose. The elements of the symmetric, square matrices $\underset{\sim}{D}(S_{ij})$ and $\underset{\sim}{R}$ are given in the Appendix.

In preparation for integrating (54) numerically, it is convenient to normalize the θ-variations by taking $\Sigma_e(0) = 1$ and defining

$$q = \Sigma_{11}(0)/\Sigma_{22}(0) \qquad (56)$$

The nonlinear two-point boundary value problem defined by (40) through (43), (50) and (54) through (56) is solved by the shooting method. For prescribed values of α and β and assumed values of s and q, (54) is numerically integrated over $\theta > 0$ until (47) is satisfied at a certain θ_p. A check is made to determine whether or not the continuity conditions, Equation (51), are satisfied for this θ_p. If not, Newton's method is used to establish new values of s and q and the procedure is repeated until (51) is satisfied.

A predictor-corrector method was used to integrate Equation (54). If $\underset{\sim}{y}_i$ denotes the solution at $\theta = i\Delta\theta$, then $\underset{\sim}{y}_{i+1}$ at $\theta = (i+1)\Delta\theta$ can be written as

$$\underset{\sim}{y}_{i+1} = \underset{\sim}{y}_i + \underset{\sim}{y}_i' \ \Delta\theta + \underset{\sim}{c} \ \Delta\theta^2/2 \qquad (57)$$

and
$$y'_{i+1} = y'_i + \underline{c}\, \Delta\theta \ . \tag{58}$$

The coefficient vector $\underline{c}$ is determined by numerical iterations; i.e., for an assumed $\underline{c}$ (57) is substituted into (54) to determine y'_{i+1} and a new estimate for $\underline{c}$ is found from (58). This procedure is repeated until y_{i+1} agrees with its previous iterant to six significant figures. Typically two iterations were sufficient and the method proved to be stable for α as small as 0.005 whereas the finite difference technique used by Achenbach and Kanninen (1978) was found to be unstable for $\alpha < 0.1$. To commence the numerical integration $\underline{y}_0$ and $\underline{y}'_0$ are required. These can be obtained by introducing Taylor series expansions about $\theta = 0$ for $\underline{D}$, $\underline{R}$ and $\underline{y}$ into (54) and equating coefficients of θ^0 and θ^1 to zero. For the boundary conditions (41) through (43) and condition (56), $\underline{y}_0$ and $\underline{y}'_0$ are given in Appendix.

RESULTS AND DISCUSSION

The numerical solution was checked by comparing it with the known elastic solution and the quasi-static, linear strain-hardening solution of Amazigo and Hutchinson (1977). For this comparison it is not possible to consider numerically the limiting case $\beta = 0$ instead, $\beta = 0.001$ was used. The computed values of s and θ_p were found to agree with Amazigo and Hutchinson's values through four significant figures for all of the values of α that they reported; i.e. from $\alpha = .005$ to 1.0.

For a given value of α, there exists a limiting crack speed above which the numerical integration algorithm failed to converge to a non-positive value of s. This occurred whenever the crack speed was greater than the Rayleigh wave speed based upon the tangent modulus; i.e. whenever

$$\beta > 0.57 \; \alpha^{1/2}; \qquad \nu = 0.3 \quad . \tag{59}$$

where β is given by Equation (21).

Numerical values of s and θ_p for the condition of plane stress are given in Table 1 for selected values of α and β and for $\nu = 0.3$. Plots of s versus α appear in Figure 3. It is apparent from this figure that if the crack speed is less than approximately one-half of the Rayleigh wave speed based upon the tangent modulus; i.e., if

$$\beta < 0.3 \; \alpha^{1/2} \quad , \tag{60}$$

the order of the stress and strain singularity does not differ significantly from that for the quasi-static condition. The stress distributions in the loading region for $\beta = 0.25$ and $\alpha = 0.3$ are shown in Figure 4. These may be

compared with the quasi-static distributions for $\alpha = 0.3$ depicted in Figure 5. While the differences are not great, the largest difference occurs for Σ_{11}.

Numerical values of s and θ_p are summarized in Table 2 and plots of s versus α appear in Figure 6 for conditions of plane strain and $\nu = 0.3$. A comparison of Figures 3 and 6 reveals that inertia effects have a more pronounced influence upon the order of the singularity for plane strain than they do for plane stress. The plane strain distribution of stresses in the loading region are shown in Figures 7 and 8. Here differences between the quasi-static distributions of Figure 7 and the dynamic counterparts of Figure 8 are more perceptible. In both instances the high triaxiality in the loading region is readily apparent.

CONCLUSIONS

A basis for the analysis of rapid crack propagation taking direct account of crack-tip plasticity has been provided in this work. Explicit determination of the crack tip singularity and the angular position at which unloading takes place has been made for both plane stress and plane strain conditions. It was found that, in both conditions, the results are much more sensitive to the ratio of the slopes of the two portions of the bilinear stress-strain relation used then to the crack speed. This indicates that, for a singular finite element dynamic crack propagation solution procedure, only modest adjustments in the crack tip element formulation will be necessary to accommodate changes in the crack speed.

ACKNOWLEDGEMENTS

REFERENCES

Achenbach, J. D. and Kanninen, M. F.　　1978　Fracture Mechanics (edited by Perrone, N. et al.) p. 649, U. Virginia Press, Charlottesville, Va.

Achenbach, J. D. and Bazant, Z.P.　　1975　J. Appl. Mech. 42, 183.

Amazigo, J. C., and Hutchinson, J. W.　　1977　J. Mech. Phys. Solids 25, 81.

Kanninen, M. F.　　1978　Numerical Methods in Fracture Mechanics (edited by Luxmoore, A. R. and Owen, D. R. J.), U. College of Swansea Press, Swansea, U.K.

APPENDIX

The nonzero elements of the symmetric matrices $\underset{\sim}{D}$ (S_{ij}) and $\underset{\sim}{R}$ for plane strain are as follows. Note, for plane stress, the last column in $\underset{\sim}{R}$ and $\underset{\sim}{D}$ (S_{ij}) and the last row in $\underset{\sim}{R}$, $\underset{\sim}{y}$, $\underset{\sim}{y}_o$, and $\underset{\sim}{D}$ (S_{ij}) are deleted.

$$D_{11} = D_{22} = \beta^2 \sin\theta \tag{A1}$$

$$D_{13} = D_{31} = D_{25} = D_{52} = \sin\theta \tag{A2}$$

$$D_{15} = D_{51} = D_{24} = D_{42} = -\cos\theta \tag{A3}$$

$$D_{33} = \left[1 + \frac{9(1-\alpha)}{4\alpha} \frac{S_{11}^2}{\Sigma_e^2}\right] \sin\theta \tag{A4}$$

$$D_{44} = \left[1 + \frac{9(1-\alpha)}{4\alpha} \frac{S_{22}^2}{\Sigma_e^2}\right] \sin\theta \tag{A5}$$

$$D_{55} = \left[2(1+\nu) + \frac{9(1-\alpha)}{\alpha} \frac{S_{12}^2}{\Sigma_e^2}\right] \sin\theta \tag{A6}$$

$$D_{66} = \left[1 + \frac{9(1-\alpha)}{4\alpha} \frac{S_{33}^2}{\Sigma_e^2}\right] \sin\theta \tag{A7}$$

$$D_{34} = D_{43} = -\left[\nu - \frac{9(1-\alpha)}{4\alpha} \frac{S_{11} S_{22}}{\Sigma_e^2}\right] \sin\theta \tag{A8}$$

$$D_{35} = D_{53} = \frac{9(1-\alpha)}{2\alpha} \frac{S_{11} S_{12}}{\Sigma_e^2} \sin\theta \tag{A9}$$

$$D_{36} = D_{63} = -\left[\nu - \frac{9(1-\alpha)}{4\alpha} \frac{S_{11} S_{33}}{\Sigma_e^2}\right] \sin\theta \tag{A10}$$

$$D_{45} = D_{54} = \frac{9(1-\alpha)}{2\alpha} \frac{S_{22} S_{12}}{\Sigma_e^2} \sin\theta \tag{A11}$$

$$D_{46} = D_{64} = -\left[\nu - \frac{9(1-\alpha)}{4\alpha} \frac{S_{22} S_{33}}{\Sigma_e^2}\right] \sin\theta \tag{A12}$$

$$D_{56} = D_{65} = \frac{9(1-\alpha)}{2\alpha} \; \frac{S_{33} \, S_{12}}{\Sigma_e^{\;2}} \, \sin\theta \tag{A13}$$

$$R_{11} = R_{22} = - \, s\beta^2 \cos\theta \tag{A14}$$

$$R_{13} = R_{31} = R_{25} = R_{52} = - \, s\cos\theta \tag{A15}$$

$$R_{15} = R_{51} = R_{24} = R_{42} = - \, s\sin\theta \tag{A16}$$

$$R_{33} = R_{44} = R_{66} = - \, \frac{s}{\alpha} \cos\theta \tag{A17}$$

$$R_{34} = R_{43} = R_{36} = R_{63} = R_{46} = R_{64} = s\left(\frac{1-\alpha}{2\alpha} + \nu\right) \cos\theta \tag{A18}$$

$$R_{55} = - \, s\left[2(1 + \nu) + \frac{3(1-\alpha)}{\alpha}\right] \cos\theta \quad . \tag{A19}$$

The values of $\underset{\sim}{y}$ and $\underset{\sim}{y}'$ at $\theta = 0$ are

$$\underset{\sim}{y}_o^{\,T} = \Sigma[a,\; o,\; q,\; 1,\; o,\; g] \tag{A20}$$

and

$$\underset{\sim}{y'}_o^{\,T} = \Sigma[o,\; b,\; o,\; o,\; c,\; o] \tag{A21}$$

where

$$\Sigma = (1 + q^2 + g^2 - q - qg - g)^{-1/2} \tag{A22}$$

$$a = (g + 1)\left[\frac{1-\alpha}{2\alpha} + \nu\right] - \frac{q}{\alpha} \tag{A23}$$

$$b = s(g + q)\left[\frac{1-\alpha}{2\alpha} + \nu\right] - \frac{s}{\alpha} \tag{A24}$$

$$c = -s\,(\beta^2 a + q) \tag{A25}$$

$$g = \alpha(a + 1)\left[\frac{1-\alpha}{2\alpha} + \nu\right] \quad . \tag{A26}$$

TABLE 1. PLANE STRESS RESULTS

$\alpha \backslash \beta$	0.1	0.25	0.40	0.5
		s		
1.0	−0.500	−0.500	−0.500	−0.500
0.7	−0.460	−0.457	−0.439	
0.5	−0.419	−0.411	−0.371	
0.3	−0.355	−0.339		
0.2	−0.306	−0.282		
0.1	−0.232			
		θ_p		
1.0	1.408	1.496	1.706	0.750
0.7	1.426	1.516	1.712	
0.5	1.425	1.517	1.719	
0.3	1.401	1.498		
0.2	1.370	1.475		
0.1	1.304			

TABLE 2. PLANE STRAIN RESULTS

$\alpha \backslash \beta$	0.1	0.25	0.40	0.5
		s		
1.0	−0.500	−0.500	−0.500	−0.500
0.7	−0.472	−0.468	−0.445	
0.5	−0.440	−0.426	−0.336	
0.3	−0.369	−0.320		
0.2	−0.292	−0.161		
0.1	−0.180			
		θ_P		
1.0	1.550	1.630	1.771	0.602
0.7	1.624	1.699	1.798	
0.5	1.718	1.768	1.834	
0.3	1.871	1.847		
0.2	1.967	1.802		
0.1	2.091			
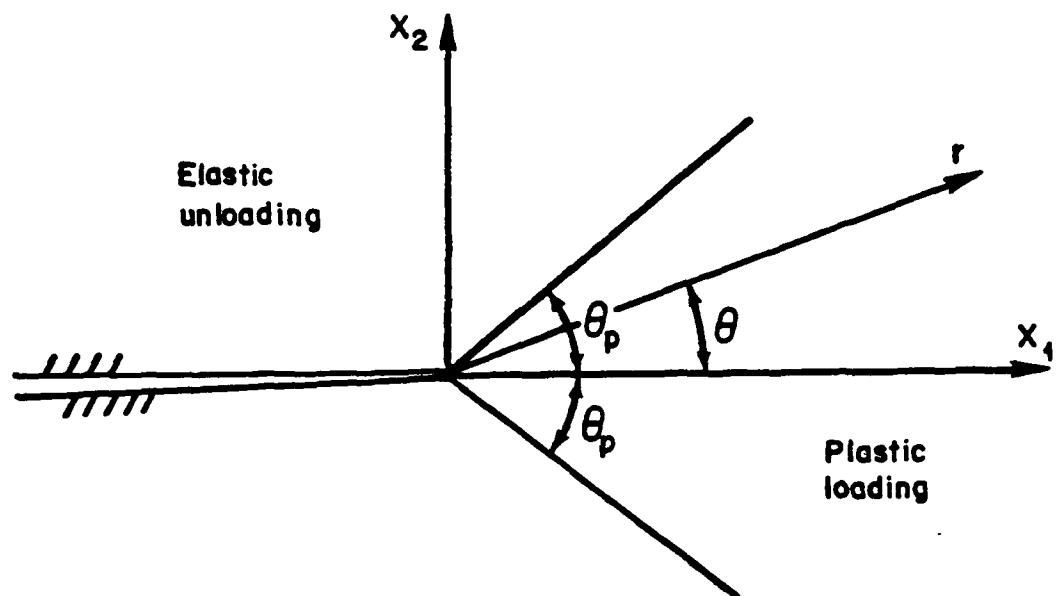
FIGURE 1.   CRACK TIP GEOMETRY
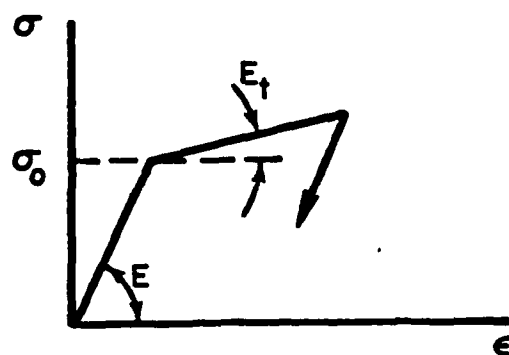
FIGURE 2.   BILINEAR STRESS-STRAIN CURVE
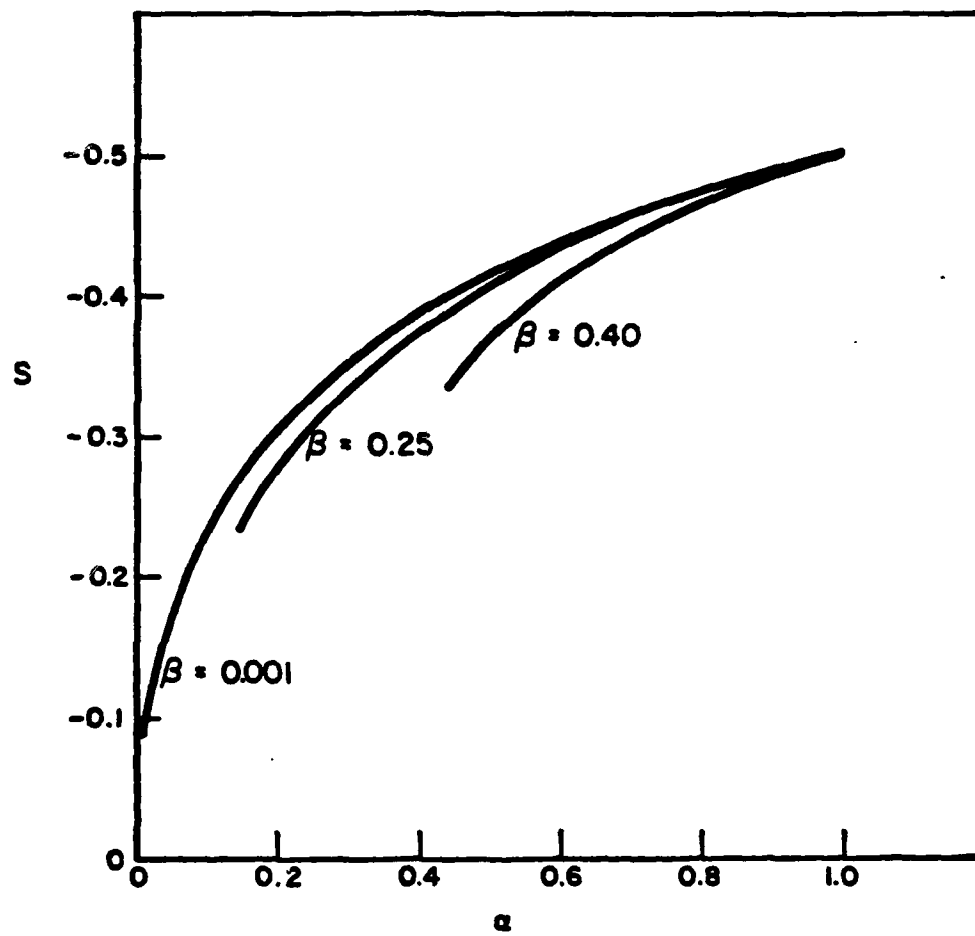
FIGURE 3. ORDER OF THE CRACK TIP SINGULARITY IN PLANE STRESS
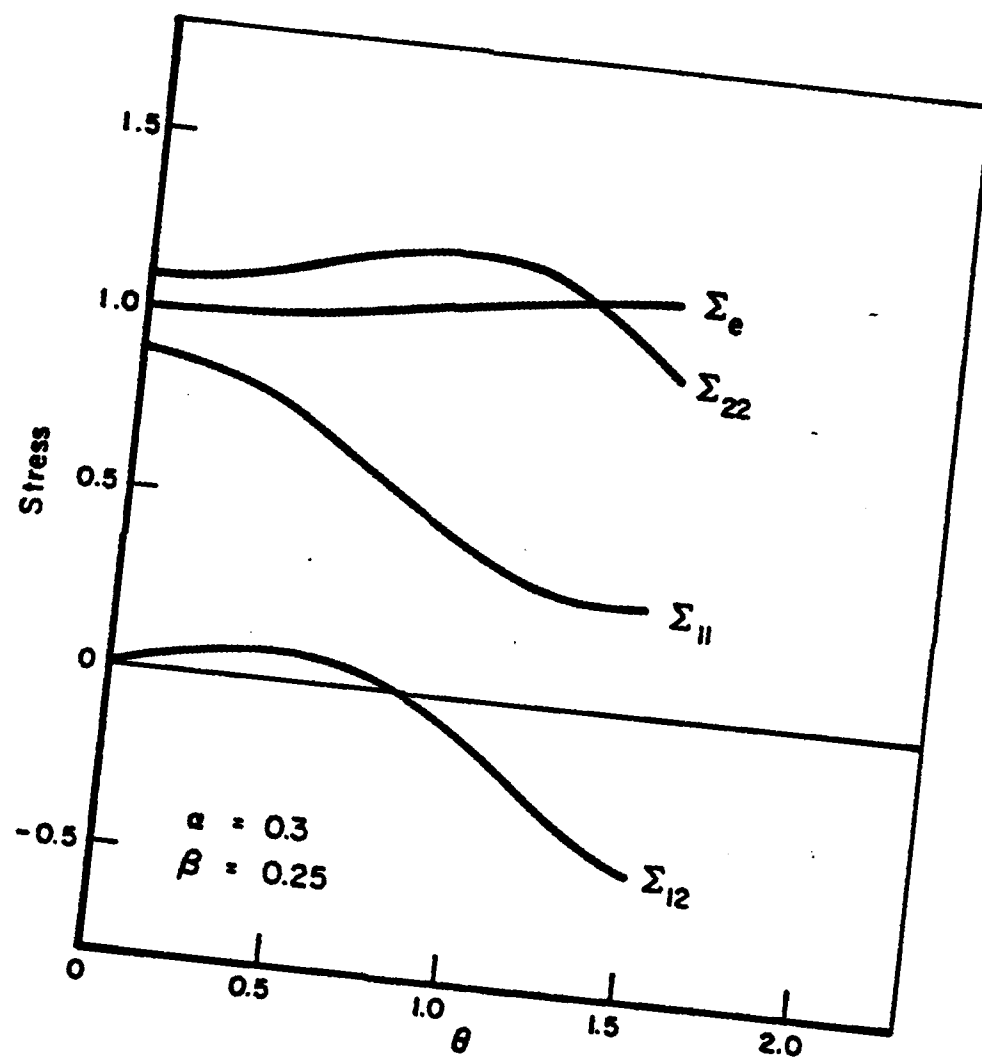
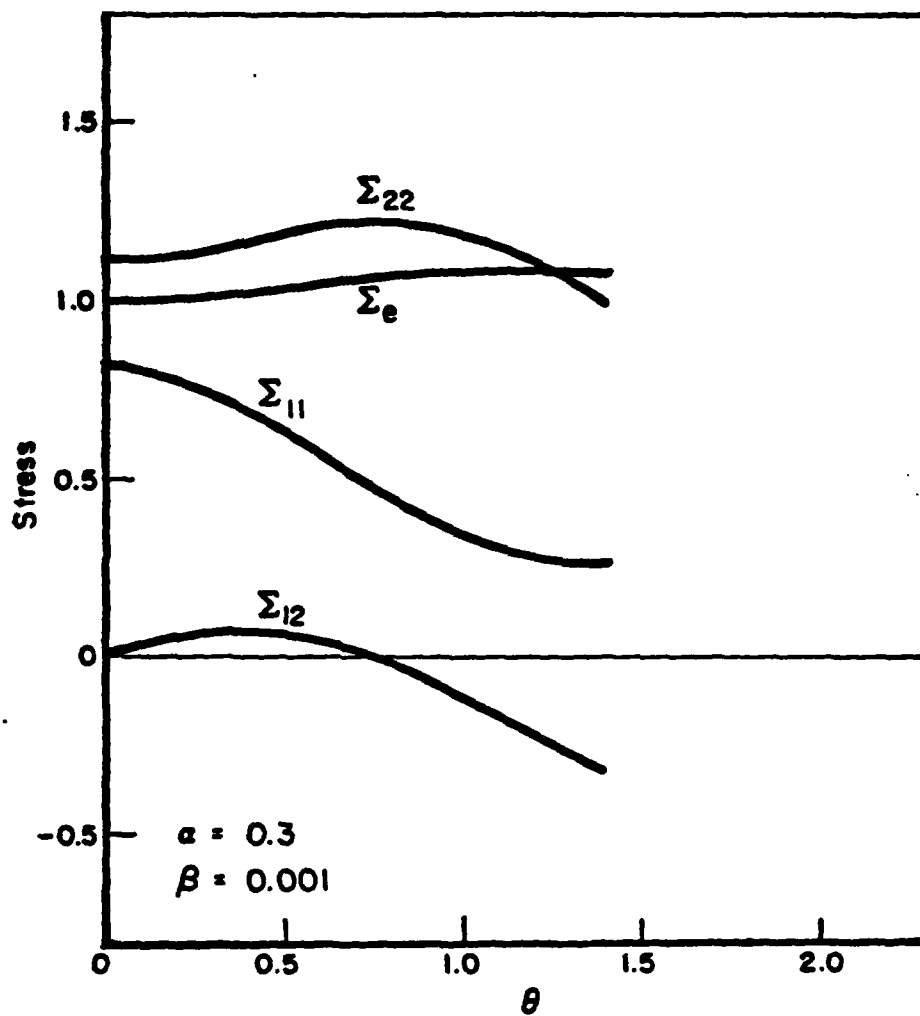FIGURE 4. DYNAMIC CRACK TIP STRESSES IN PLANE STRESS

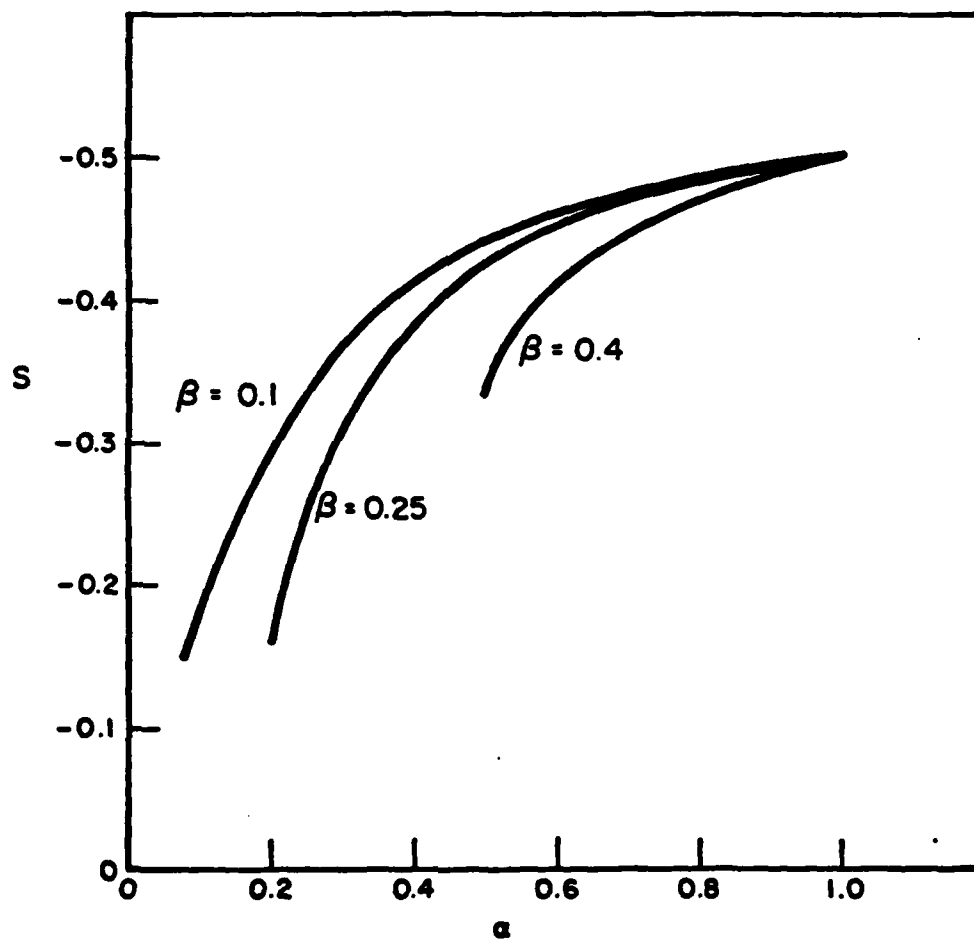FIGURE 5.   QUASI-STATIC CRACK TIP STRESSES IN PLANE STRESS

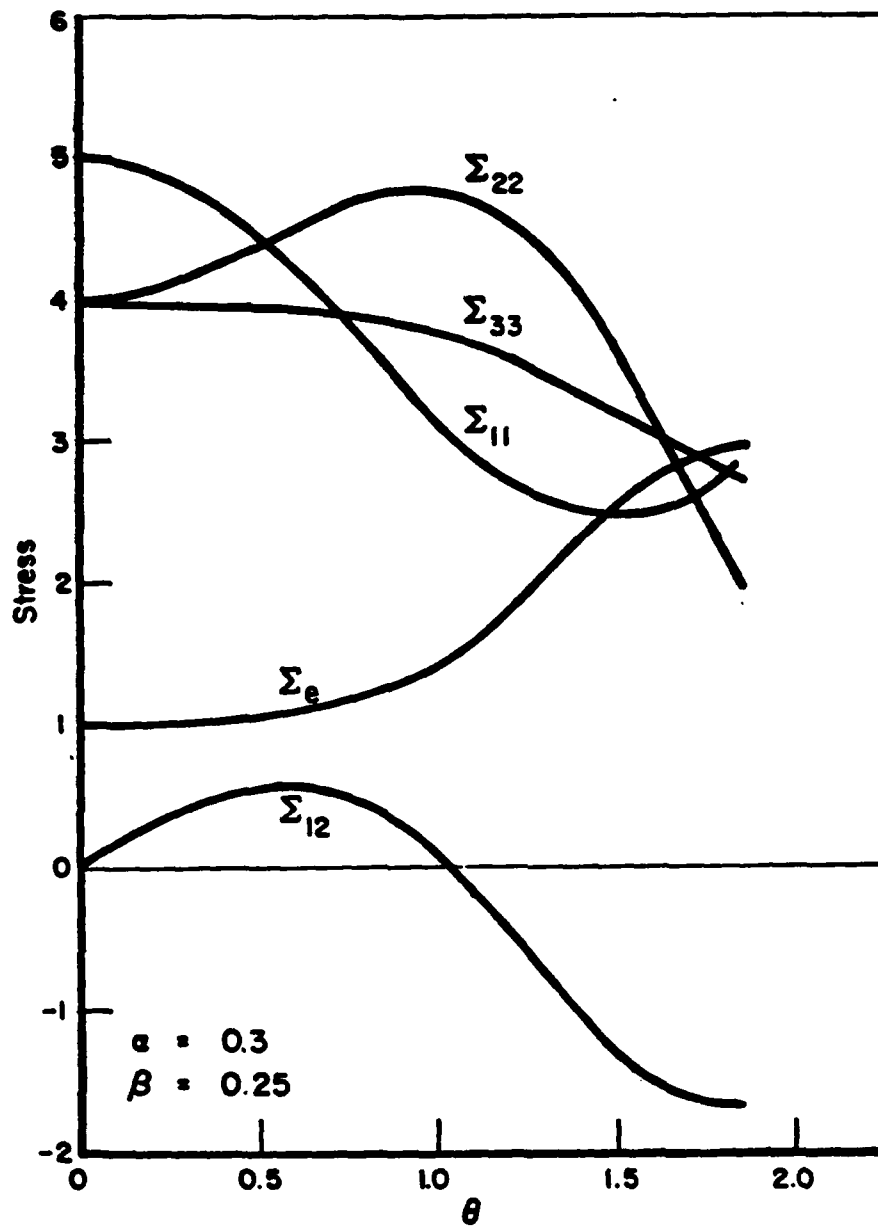FIGURE 6. ORDER OF THE CRACK TIP SINGULARITY IN PLANE STRAIN
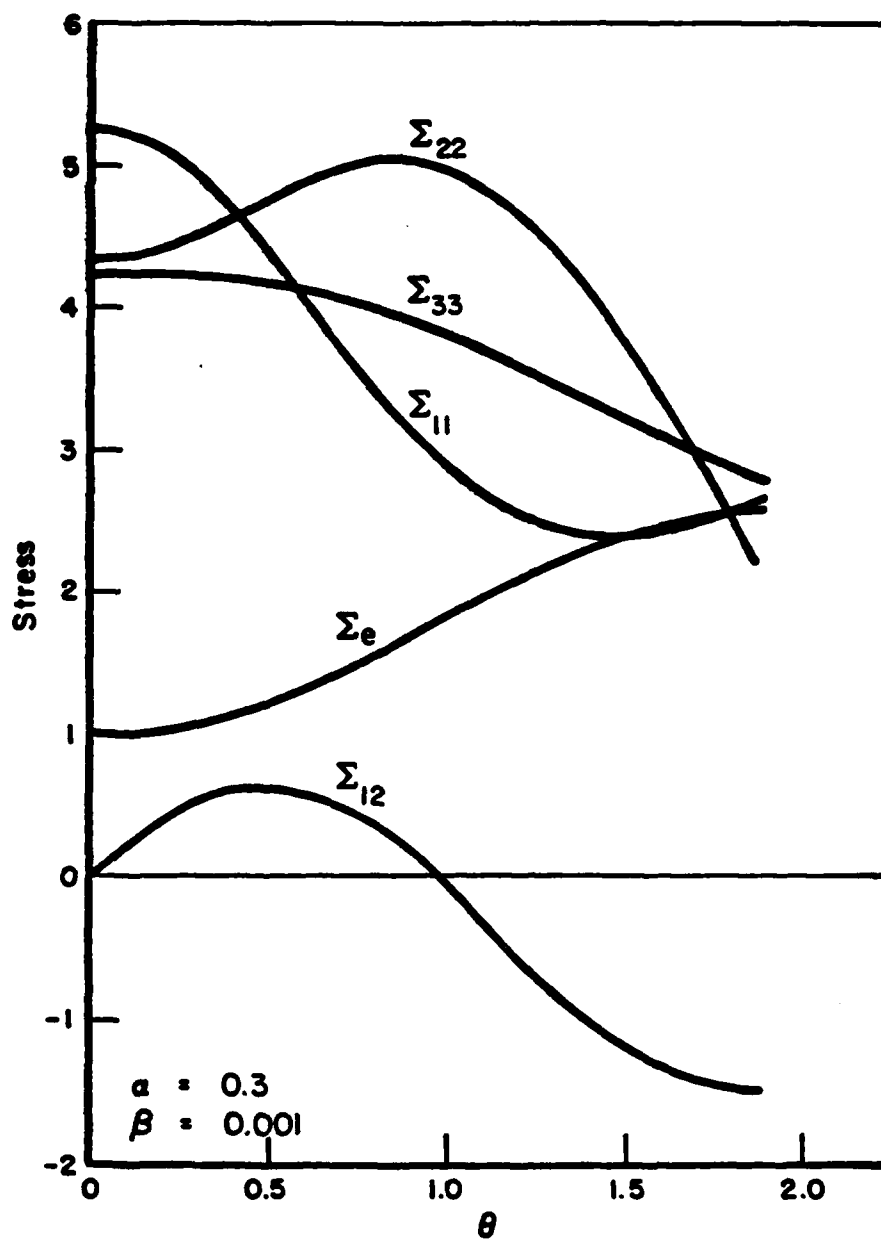
FIGURE 7. DYNAMIC CRACK TIP STRESSES IN PLANE STRAIN

FIGURE 8.   QUASI-STATIC CRACK TIP STRESSES IN PLANE STRAIN